Root malformation associated with a cervical mineralized diaphragm − a distinct form of tooth abnormality?

Catherine Victoria Amirtham Witt, BDS, MClinDent,[a] Thomas Hirt, DMD,[b] Gordian Rutz, DMD,[c] and Hans Ulrich Luder, DMD, PhD[d]

Private Practice, Büsingen, Switzerland; Private Practice, Uster, Switzerland; and Center of Dental Medicine, University of Zurich, Zurich, Switzerland

Objective. Deviations in length and shape of tooth roots result from hard tissue resorption or occur as a developmental disorder. The purpose of this report is to present a type of root malformation which seems to have gone unreported so far.

Study design. Two patients showing severely dysplastic roots of all permanent first molars were evaluated using radiography, histology as well as scanning and transmission electron microscopy.

Results. Medical histories of the patients revealed significant, but diverse events in the first year after birth. Radiographically the pulp cavity floors of the affected molars in large part were occupied by ectopic mineralized plates. Microscopically these plates consisted of hard tissue, densely calcified globules, and a network of canals which contained large blood vessels and were lined by cementum and periodontal ligament.

Conclusions. We propose that the ectopic mineralized plate was derived from the dental follicle, had developed during crown formation around the vascular plexus at the base of the dental papilla, and represented a mechanical obstacle interfering with normal root development. (Oral Surg Oral Med Oral Pathol Oral Radiol 2014;117:e311-e319)

Short or absent tooth roots most frequently result from hard tissue resorption as a sequel to dento-periodontal traumas, orthodontic tooth movements, local inflammatory processes, tumors, and endocrine disorders.[1,2] More rarely, however, radicular dysplasias can also occur as a developmental disorder involving either a primary disruption or premature arrest of normal root formation. Primary disruption of radicular development is associated with dentin dysplasia type I[3-5] and regional odontodysplasia.[6,7] In these conditions, the root dysplasia is generalized or affects a continuous section of a dental arch. Premature arrest of radicular development results from local events such as trauma, infection, radiation therapy, systemic influences like chemotherapy,[8-10] and sometimes without any apparent reason.[11] Therefore, this type of dysplasia usually affects individual teeth or a specific group of teeth, the roots of which were forming at the time of the external insult.

The aim of this report is to present a type of root malformation detected in two unrelated patients, which does not fit in any of the above categories and seems to have gone unreported so far.

MATERIALS AND METHODS

Patients

Two patients presenting a radiographically very similar, severe root malformation of all four permanent first molars were detected incidentally. The first patient, a boy born in Germany of Macedonian parents, was referred to a pediatric dentist at the age of 8 years 1 month for the treatment of deep caries of primary and permanent teeth. At that time, the boy was healthy, but the mother reported that at the age of 9 months he had been admitted to a hospital because of a severe infection of the left thigh. Medical records obtained from the clinic revealed an osteomyelitis of the left femur head with involvement of the soft tissues due to an infection with *Staphylococcus aureus*. The in-patient treatment consisted of intravenous administration of a combination of a cephalosporine (Cefuroxim; Sandoz Pharmaceuticals, Rotkreuz, Switzerland) for 5 days, a penicillin (Flucloxacillin; OrPha Swiss, Küsnacht, Switzerland) for 5 weeks, a lincosamide (Clindamycin; Pfizer, Zurich, Switzerland) for 5 weeks, and a glycopeptide antibiotic (Vancomycin; Pfizer) for 4 weeks. Recovery after dismissal from the hospital was free of complications, and several follow-up examinations over almost 2 years did not disclose any permanent damage of the hip joint.

In addition to bite-wing radiographs, the pediatric dentist exposed a panoramic radiograph to assure that all permanent teeth were present. The first permanent molars were extracted and the primary molars restored under general anesthesia. With informed consent of the parents, the extracted teeth were examined by X-ray microtomography (microCT), light microscopy (LM), backscattered scanning (BSE), and transmission electron microscopy (TEM).

The second patient, a girl of Swiss descent, was 10.5 years old when a panoramic radiograph was taken for orthodontic treatment planning disclosed the root malformation of all permanent first molars. The medical history obtained from the father revealed that

[a]Clinician, Private Practice, Büsingen, Switzerland.
[b]Clinician, Private Practice, Uster, Switzerland.
[c]Lecturer, Department of Orthodontics, Center of Dental Medicine, University of Zurich.
[d]Professor, Institute of Oral Biology, Center of Dental Medicine, University of Zurich.

Received for publication May 9, 2013; returned for revision Jun 12, 2013; accepted for publication Jun 25, 2013.

2212-4403/$ - see front matter
http://dx.doi.org/10.1016/j.oooo.2013.06.030

a relatively advanced astrocytoma of the mother, diagnosed during the 34th week of pregnancy, had necessitated a premature delivery by a Caesarean section in the 36th week. Thereafter, treatment of the tumor with oral doses of a corticosteroid was initiated, but the mother insisted on breast-feeding her daughter. Two months later she had to stop breast-feeding, and when the child was 3 years old, the mother died. Further medical history of the girl only revealed relatively frequent middle ear infections which started at about 2 years of age and were mostly treated with a combination of amoxicillin and clavulanic acid (Augmentin; GlaxoSmithKline, Münchenbuchsee, Switzerland) orally for no longer than 1 week.

After noting the abnormal roots, cone beam computed tomography (CBCT) scans of all permanent first molars were taken at the age of 13 years 3 months. Using a Veraviewepocs 3D device (J. Morita MFG Corp., Dietzenbach, Germany), four cylindrical volumes with a diameter of 42.625 mm and a height of 43.0 mm were scanned at a slice thickness of 1.5 mm and a slice interval of 1.0 mm. Three-dimensional reconstructions were made at a voxel size of 0.125 mm using the proprietary i-Dixel One Volume Viewer V2.0 (J. Morita MFG Corp., Dietzenbach, Germany). In addition, image data of individual slices in bmp-format were imported in the program VGStudio Max (Volume Graphics, Heidelberg, Germany), which was used to manually segment the various hard tissues and, thus, to isolate the teeth and view their roots.

MicroCT evaluation and histologic processing

All four permanent molars removed from patient 1 were fixed in a mixture of 4% paraformaldehyde and 0.2% glutaraldehyde in 0.1 M phosphate buffer (pH 7.2). Following a rinse in 0.185 M Na-cacodylate buffer (pH 7.2), they were photographed using a M420 macroscope (Leica Microsystems, Heerbrugg, Switzerland) and scanned in a μCT 40 microtomograph (Scanco Medical, Brüttisellen, Switzerland). Slices of 20 μm in thickness were imaged at a resolution of 1024 × 1024 px. After image data in raw-format had been imported in VGStudio Max, the radiographs were manually segmented, distinguishing enamel, dentin, pulp cavity, and root canals as well as an ectopic hard tissue plate at the level of the cementoenamel junction (CEJ). By applying color codes to and varying the transparency of these components, it was possible to visualize their natural spatial relationship.

Following the microCT evaluation, teeth were divided in two halves using a diamond band saw (EXAKT, Norderstedt, Germany). Maxillary molars were cut in a bucco-lingual and mandibular molars in a mesio-distal direction. One half of each specimen was left fully mineralized and processed for examination in the scanning electron microscope (SEM), whereas the other half was decalcified for 2 months in 10% EDTA containing 0.2% glutaraldehyde and processed for examination in the LM or TEM.

LM evaluation

Decalcified specimens from patient 1 were dehydrated in ethanol, transferred to xylol, and embedded in methyl-methacrylate (MMA). Serial sections were cut at a thickness of 5-7 μm using a Leica RM2255 microtome (Biosystems, Nunningen, Switzerland) and tungsten-carbide knives. Sections were deplasticized and stained with toluidine blue, resorcin-fuchsin, or alcian blue (pH 2.5)-nuclear fast red. Overview micrographs were recorded with the M420 macroscope and a ProgRes C14 + camera (Jenoptik, Jena, Germany), while a DM 6000 B microscope equipped with a DFC 420 C camera (Leica Microsystems) served for preparing detail micrographs.

SEM evaluation

Fully mineralized tooth halves from patient 1 were dehydrated in ethanol and embedded in Technovit 7200 VLC (Heraeus Kulzer, Wehrheim, Germany). Light-polymerized blocks were mounted on aluminum stubs, polished, and coated with a 10-15 nm thick layer of carbon.[12] Thereafter, they were examined using a Tescan VEGA TS5316 XM SEM (Tescan, Brno, Czech Republic) operated in BSE mode. Micrographs were recorded at 20 kV and a working distance of 23 mm. In addition, mineral densities of the ectopic hard tissue plates and, as an internal control, of enamel and dentin were estimated based on BSE signal intensities.[12] Finally, the elemental composition of the same sites was analyzed with the aid of energy-dispersive X-ray spectroscopy (EDS). A Si(Li) detector (Oxford Instruments, Wiesbaden, Germany) served for recording EDS spectra using an accelerating voltage of 7 kV, a working distance of 23 mm, and a counting time of 100 s. For the quantitative evaluation of these spectra, the Inca energy software (Oxford Instruments) was used. Both mineral densities and elemental compositions obtained from the various locations were compared using analyses of variance with repeated measurements contained in the SPSS software V20 (IBM, Armonk, NY, USA).

TEM evaluation

Decalcified tooth halves from patient 1 were further cut into smaller pieces comprising particularly the ectopic hard tissue plate. These blocks were postfixed in 1.33% Os-tetroxide in 0.067 M s-collidine buffer for 2 h at room temperature. Thereafter, they were dehydrated in ethanol, transferred to propylene oxide, and embedded in Epon 812 (Fluka, Buchs, Switzerland). From the resin blocks, thin sections of 80-100 nm in thickness

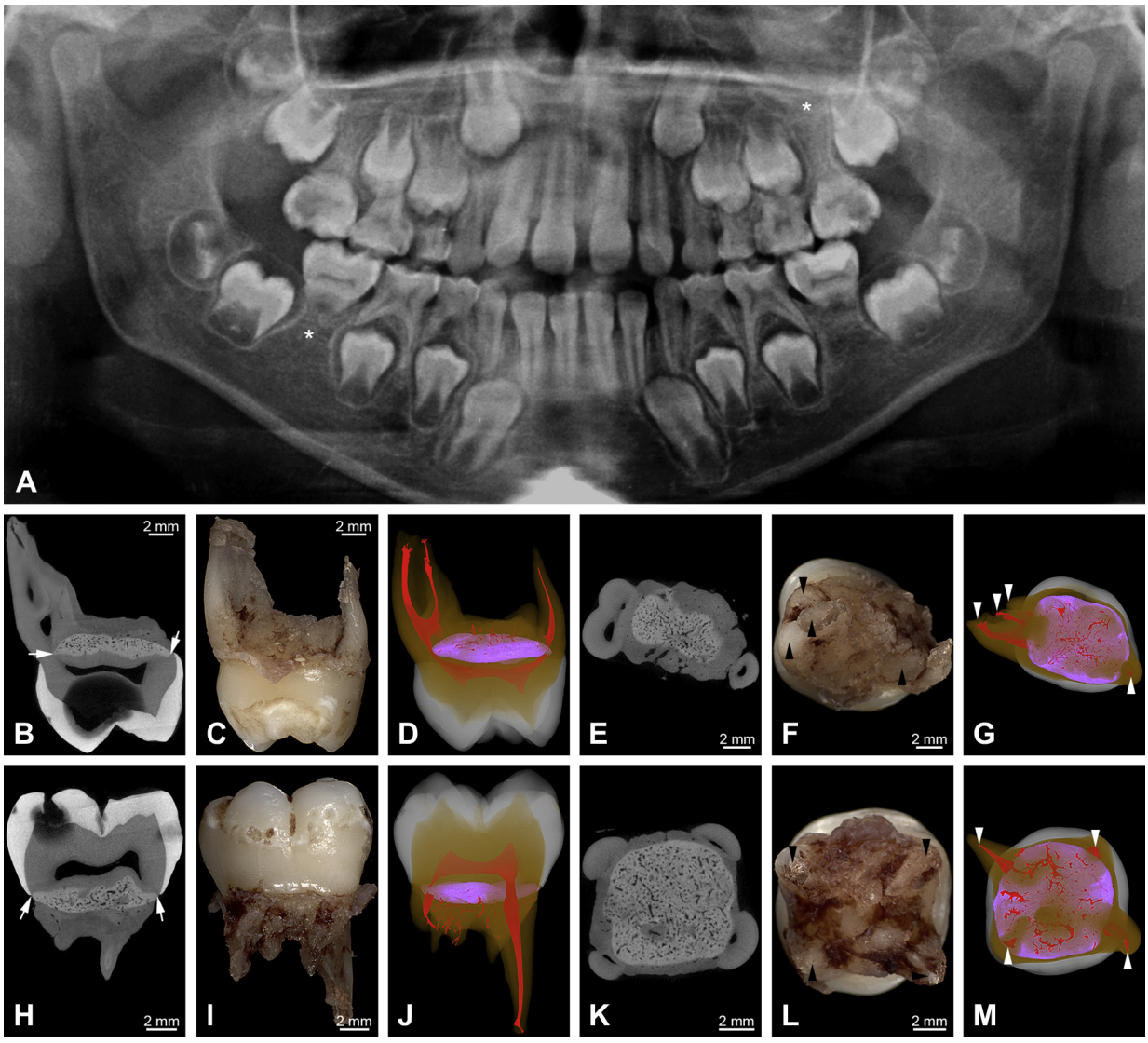

Fig. 1. Radiographic and macroscopic appearance of the permanent first molars of patient 1. (**A**), Panoramic radiograph taken at the age of 8 years 1 month [asterisks mark the permanent upper left and lower right first molars, which are shown in detail in (**B**)-(**G**) and (**H**)-(**M**), respectively]. (**B**)-(**G**), Bucco-lingual (**B**) and horizontal (**E**) microCT sections, mesial (**C**) and apical (**F**) macroscopic views, and mesial (**D**) and apical (**G**) microCT views of the permanent upper left first molar. (**H**)-(**M**), Mesio-distal (**H**) and horizontal (**K**) microCT sections, buccal (**I**) and apical (**L**) macroscopic views, and lingual (**J**) and apical (**M**) microCT views of the permanent lower right first molar. Arrows in (**B**) and (**H**) point at the edges of the CMD, arrow-heads in (**F**), (**G**), (**L**), and (**M**) mark the root tips, and in the microCT reconstructions [(**D**), (**G**), (**J**), and (**M**)] enamel is displayed in white, dentin in orange, the CMP in violet, and the pulp cavity, root canals and soft tissue canals of the CMD in red.

were cut using a Reichert Ultracut ultramicrotome (Leica Microsystems, Heerbrugg, Switzerland) and diamond knives (Diatome, Biel, Switzerland). Sections were collected on copper-grids, contrasted with U-acetate and Pb-citrate, and examined in a Philips EM400 T TEM (FEI, Eindhoven, The Netherlands) at 60 kV.[12] Micrographs were recorded using a Hamamatsu ORCA-HR camera (Hamamatsu Photonics, Hamamatsu, Japan) and the AMT image acquisition software (Deben, Bury St. Edmunds, UK).

RESULTS

Radiographic evaluation

The panoramic radiograph of the first patient (Figure 1*A*) revealed a mixed dentition comprising germs of all non-erupted permanent teeth. Whereas the crowns of all teeth were normal in appearance, the roots of the permanent first molars could barely be seen or were very short, tapered stumps. Due to a marked reduction in height, the pulp cavities of these teeth appeared as narrow slits. MicroCT scans (Figure 1*B*, *D*,

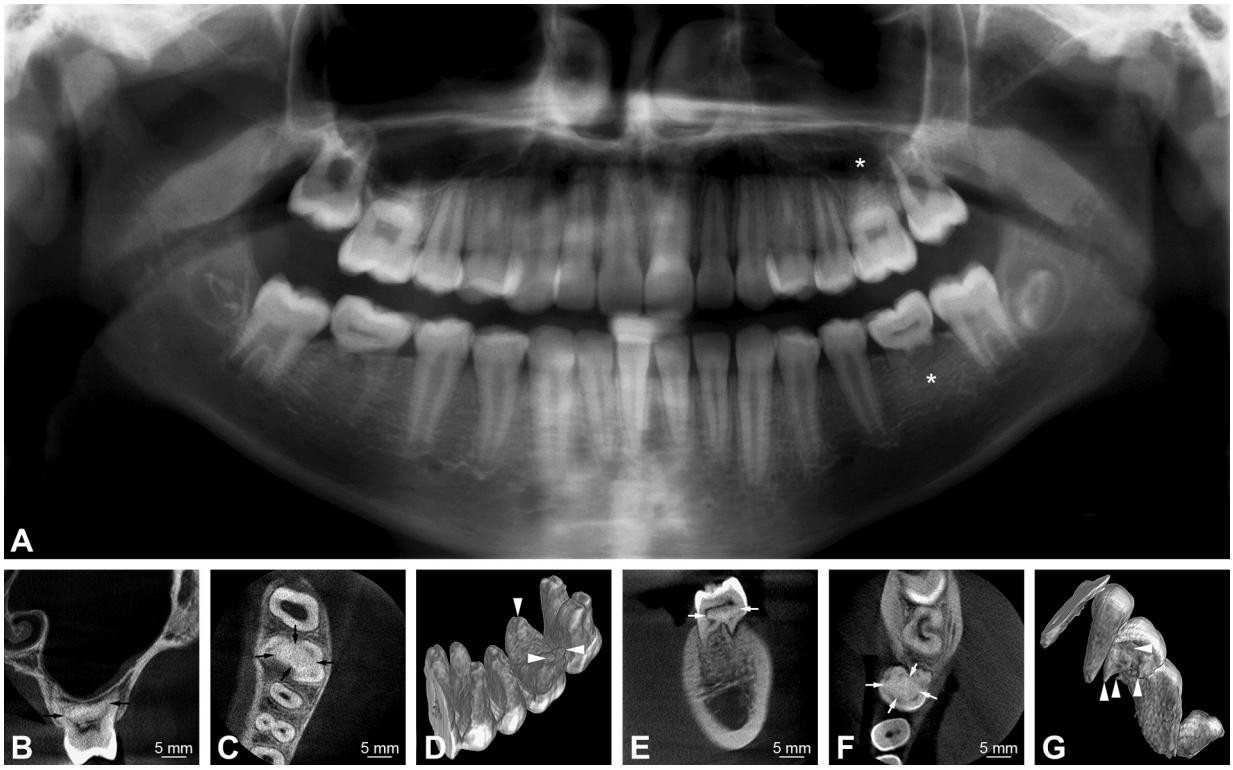

Fig. 2. Radiographic appearance of the permanent first molars of patient 2. (**A**), Panoramic radiograph taken at the age of 10 years 6 months [asterisks mark the permanent upper and lower left first molars, which are shown in detail in (**B**)-(**D**) and (**E**)-(**G**), respectively]. (**B**)-(**D**), Bucco-lingual (**B**) and horizontal (**C**) CBCT sections and mesio-bucco-apical view of CBCT reconstruction (**D**) of the permanent upper left first molar. (**E**)-(**G**), Bucco-lingual (**E**) and horizontal (**F**) CBCT sections and mesio-bucco-apical view of CBCT reconstruction (**G**) of the permanent lower left first molar. Arrows in (**B**), (**C**), (**E**), and (**F**) point at the edges of the CMD, arrow-heads in (**D**) and (**G**) mark the root tips.

E, *G*, *H*, *J*, *K*, and *M*) of the extracted molars revealed ectopic mineralized plates at the level of the CEJ, which were called cervical mineralized diaphragms (CMD). Their radiodensity was between those of enamel and dentin (Figure 1*B*, *E*, *H*, and *K*). Interspersed in the calcified matrix, they contained dense networks of delicate soft tissue canals (Figure 1*B*, *D*, *E*, *G*, *H*, *J*, *K*, and *M*). In some areas the plates extended almost to the enamel margin, but in other areas they left some space for attachments of roots (Figure 1*B* and *E*). In the maxillary molars, the two buccal roots were short and slender or only rudimentary, while the palatal root was almost normal in length and seemed to consist of two merged portions (Figure 1*B-G*). In the mandibular molars, there were always four short radicular stumps (Figure 1*H-M*). Root canals consistently exhibited curved isthmuses around the edges of the CMDs (Figure 1*D* and *J*).

In the second patient, the panoramic radiograph (Figure 2*A*) revealed an almost complete permanent dentition and first molars very similar to those of the first patient. In the maxillary molars, only the root trunk was clearly visible and in the mandibular molars, the roots were short and blunt and the pulp cavities slit-shaped. CBCT scans (Figure 2*B*, *C*, *E*, and *F*) did not disclose the outline of the CMDs as clearly as the microCT images of patient 1. However, the radio-density of the region between the roof of the furcation and the floor of the pulp cavity was consistently about 6%-11% higher (lighter) than that of the coronal dentin. The 3-dimensional reconstructions of the teeth revealed three markedly spread roots in the maxillary (Figure 2*D*) and four short, stumpy roots in the mandibular molars (Figure 2*G*). As in the first patient, root canals exhibited sharp bends at the level of the CEJ (Figure 2*E*).

Microscopic evaluation

Microscopic findings obtained from the teeth of the first patient are presented in Figures 3-5. Histological sections (Figure 3*A*) showed that the coronal dentin was normal. Dentinal tubules under smooth tooth surfaces followed an S-shaped course in an apical direction (Figure 4). When a more or less regular root adjoined to coronal dentin, the outer radicular surface was covered by acellular cementum, and the root dentin contained

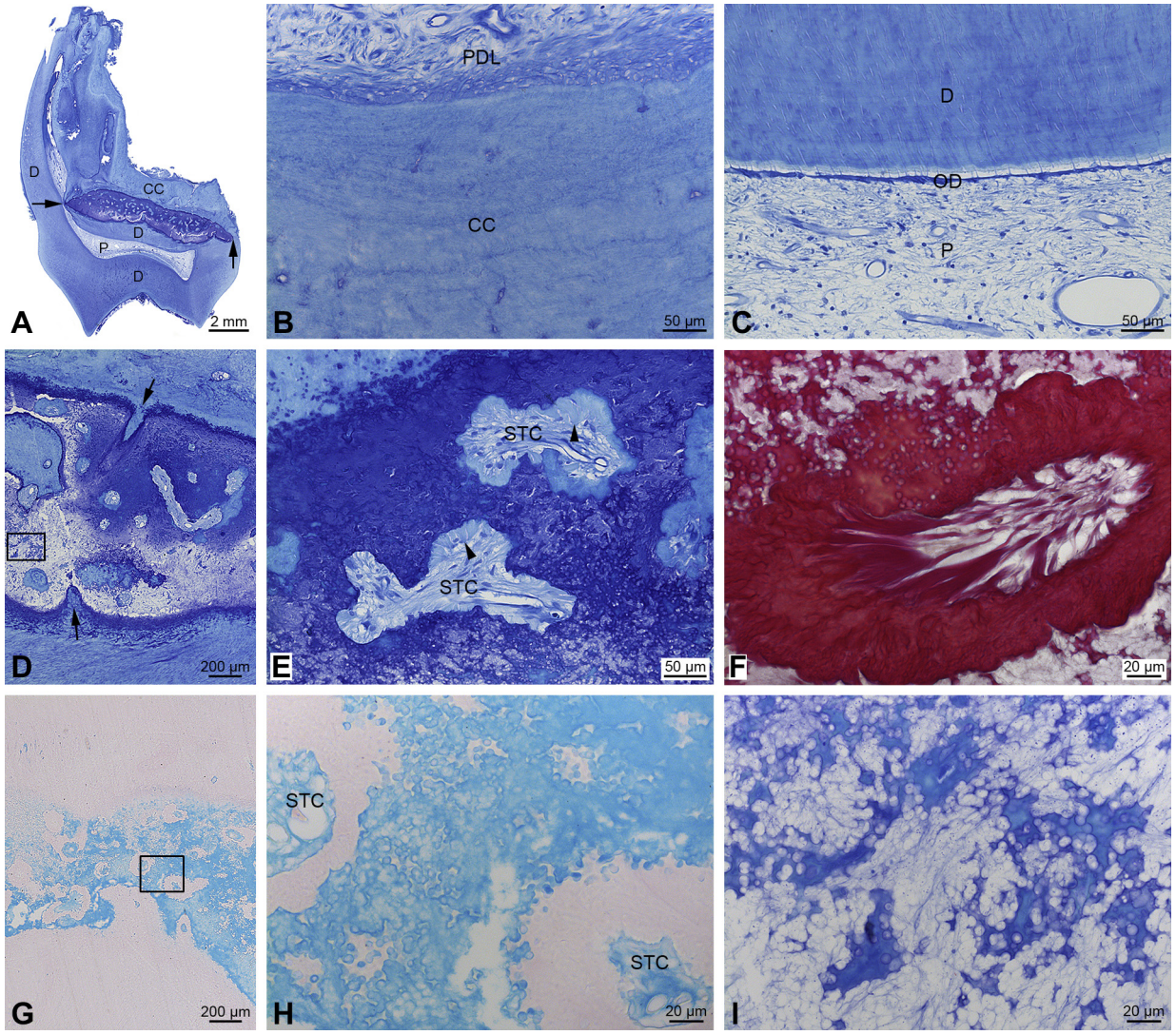

Fig. 3. Light microscopic appearance of the permanent upper left first molar of patient 1. (**A**), Bucco-lingual overview (arrows indicate the edges of the CMD). (**B**), Roof of the furcation. (**C**), Floor of the pulp cavity. (**D**), Overview of the central part of the CMD (arrows point at openings of soft tissue canals, the rectangle marks the detail I). (**E**), Closer view of two soft tissue canals (STC) in the CMD (arrow-heads point at collagen fiber bundles inserting in the canal walls). (**F**), Detail of a soft tissue canal with a mineralized lining and anchored collagen fiber bundles. (**G**), Overview of the CMD corresponding approximately to (**D**) [the rectangle marks the detail (**H**)]. (**H**) and (**I**), Details of the CMD showing the calcified globules and interglobular matrix. *CC*, cellular cementum; *D*, dentin; *OD*, odontoblasts; *P*, pulp; *PDL*, periodontal ligament; *STC*, soft tissue canals. (**A**)-(**E**) and (**I**), toluidine blue; (**F**), resorcin-fuchsin; (**G**) and (**H**), alcian blue (pH 2.5)-nuclear fast red. Original magnifications (**A**), 4×; (**D**) and (**G**), 40×; (**B**), (**C**), and (**E**), 160×; (**F**), (**H**), and (**I**), 320×.

tubules running a normal course toward the root canal. However, when the CMD extended more closely to the enamel margin, dentinal tubules changed their course in a coronal direction and ran almost horizontally along the border of the CMD toward the pulp cavity (Figure 4). Correspondingly, the floor of the pulp cavity consisted of dentin lined by a layer of predentin and flat odontoblast-like cells (Figure 3*C*). In contrast, the roof of the furcation comprised only cellular cementum and attached periodontal ligament (PDL; Figure 3*B*).

The CMD was composed of densely calcified globules of about 2-3 µm in diameter interspersed in a moderately mineralized matrix (Figure 3*I* and Figure 5*B-F*), which was traversed by a dense network of soft tissue canals (Figure 3*D-F* and Figure 5*B*). These canals seemed to enter the plate from both the apical and coronal surface (Figure 3*D*) and mostly contained prominent blood vessels (Figure 3*E*). These were frequently lined by a mineralized tissue resembling root cementum (Figure 3*F* and Figure 5*B* and *C*), into which

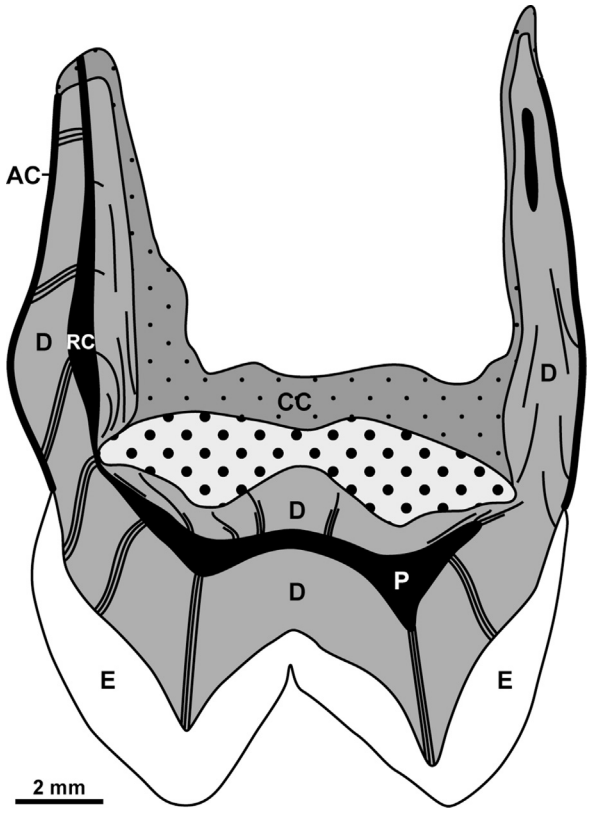

Fig. 4. Hard and soft tissue arrangement around the CMD. Schematic representation of a bucco-lingual section corresponding approximately to those displayed in Figure 3*A* and Figure 5*A*, which shows the tissue distribution (*AC*, acellular cementum; *CC*, cellular cementum; *D*, dentin; *E*, enamel; *P*, pulp; *RC*, root canal) and the course of the dentinal tubules in various regions around the CMD (black-dotted area).

inserted bundles of collagen fibers similar to those of the PDL (Figure 3*E* and *F*). The calcified globules occurred sometimes singly, but often coalesced and occasionally formed aggregates in which individual constituents could not be identified any more (Figure 5*B-F*). Individual globules or those in small clusters revealed a densely calcified periphery and a moderately calcified core (Figure 5*B* and *C*).

Overall, the mineral density of the globular part of the CMD significantly ($P < .01$) exceeded that of peritubular dentin, whereas the hard tissue lining the soft tissue canals and the interglobular matrix were mineralized less densely ($P < .05$) than coronal intertubular dentin. In contrast, Ca/P molar ratios reflecting the nature of the constituent mineral did not differ significantly ($P > .05$) between regular dental hard tissues and either component of the CMD (Table I). The inhomogeneous calcification pattern of the globules corresponded well to an intense peripheral as opposed to only light central staining with alcian blue at pH 2.5 (Figure 3*G* and *H*). A similar difference could also be observed in decalcified TEM preparations with respect to the electron contrast. While individual globules or small clusters revealed a thin, very electron-dense surface lamina and a core composed of minute granules (Figure 5*D*), these granules were mainly concentrated in the periphery of globules occurring in larger clusters (Figure 5*E*).

DISCUSSION

The similar radiographic findings obtained from two unrelated patients suggest that the observed root malformation associated with a CMD represents a distinct form of dysplasia which, to the best of our knowledge, has not been described so far. In contrast to the situation in regional odontodysplasia,[6,7] the crowns of the affected teeth are normal, and unlike in dentin dysplasia type I,[3,4,13] the pulp cavities are not obliterated. The newly observed malformation could also be mistaken for a consequence of severe root resorption. However, the two conditions can be clearly distinguished based on the characteristic radiographic signs of the root dysplasia. These are short, tapering roots associated with a conspicuous slit-shaped pulp cavity and, if visible, an abnormally coronal position of the furcation, so to say an inverse taurodontism.

It should be noted that deep dentin caries, rather than compromised tooth support, was the reason to extract all four first permanent molars in the first patient. Similarly, periodontal status was excellent in the second patient as well. Therefore, a CBCT evaluation using the best available resolution was made in this case, whereas in the first patient, the extractions enabled also a microscopic analysis.

As far as the potential etiology of the root malformation is concerned, a genetic cause cannot be completely excluded, because several forms of short or absent roots in mice have recently been shown to be due to defects in various genes, including the *Nfic* gene,[14] the *Ptc* gene,[15] and the *Dkk1* gene.[16] However, none of these abnormalities affected only one type of tooth, and all lacked the typical feature of the CMD. Therefore, an external adverse effect active during the development of the permanent first molars seems a more likely explanation for the root malformation in our patients, although the medical histories regarding the potential causative factor were unproductive. The only common feature was a relatively dramatic event during the first year of postnatal life.

In the first case, a severe infection at the age of 9 months was treated with a combination of several antibiotics, which notably did not include amoxicillin, as the causative microorganism proved to be resistant. Amoxicillin seems to be the only antibiotic, of which potential adverse effects on tooth development have been reported.[17,18] The situation in the second patient is

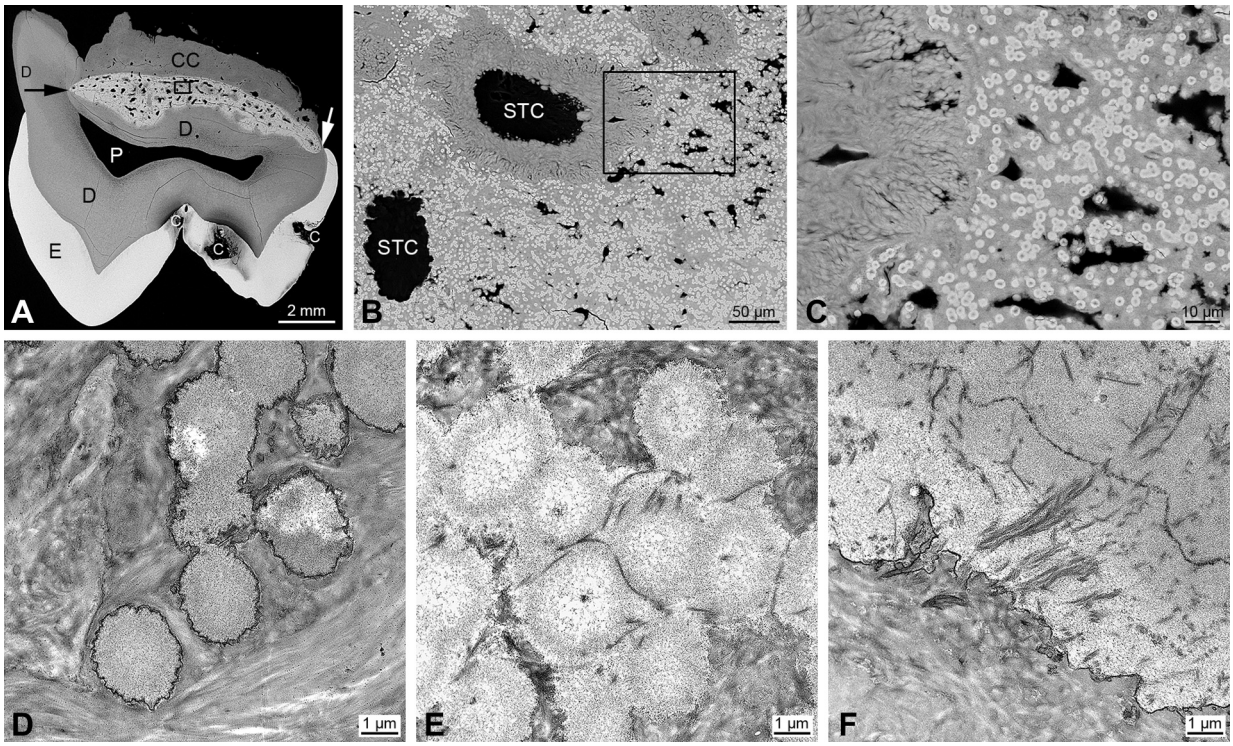

Fig. 5. Backscattered (**A**)-(**C**) and transmission (**D**)-(**F**) electron microscopic appearance of the CMD in the permanent upper left first molar of patient 1. (**A**), Bucco-lingual overview (arrows point at the edges of the CMD, the rectangle marks the detail (**B**), *C*, caries; *CC*, cellular cementum; *D*, dentin; *E*, enamel; *P*, pulp cavity). (**B**), Closer view of two soft tissue canals (STC) in the CMD [the rectangle marks the detail (**C**)]. (**C**), Detail of the wall of a soft tissue canal as well as of the mineralized globules and interglobular matrix of the CMD. (**D**)-(**F**), High magnifications of loosely arranged (**D**), densely packed (**E**), and completely fused (**F**) globules embedded in the collagenous interglobular matrix of the CMD. Original magnifications (**A**), 40×; (**B**), 1500×; (**C**), 5000×; (**D**)-(**F**), 13,000×.

Table I. Mineral densities and calcium/phosphate (Ca/P) molar ratios estimated in the two mineralized components of the CMD and, as an internal control, in enamel and dentin of patient 1

Hard tissue	*Measurement*	*Mean*	*Range*
CMD (globular part)	Mineral density (%)	85.4	84.7-86.0
	Ca/P molar ratio	1.37	1.31-1.39
CMD (interglobular part)	Mineral density (%)	60.6	59.4-61.4
	Ca/P molar ratio	1.34	1.31-1.38
Internal control			
Enamel	Mineral density (%)	100.0*	97.2-102.8
	Ca/P molar ratio	1.35	1.34-1.36
Intertubular dentin	Mineral density (%)	65.6	63.8-66.6
Peritubular dentin	Mineral density (%)	77.2	74.4-79.6
Dentin†	Ca/P molar ratio	1.31	1.27-1.35

*Please note that in comparison with the chemical composition, this value is slightly overestimated, because the samples were dehydrated and, therefore, no water content was taken into account.
†The spatial resolution of the EDS detector was insufficient to discriminate inter and peritubular dentin.

even more obscure. This girl ingested a corticosteroid with mother's milk during 2 months of breast-feeding immediately after birth. It is known that levels of corticosteroids in breast milk are usually less than 50% of those in serum.[19] Furthermore, the duration of the intake was short and no immediate clinical side-effects were noticed in our patient. As an alternative hypothesis, the astrocytoma of the mother could have affected tooth development of the child during late pregnancy. However, there are no precedents to support this possibility. Finally, the amoxicillin utilized for treating the ear infections is unlikely to be the causative agent for the root malformation, because the use of amoxicillin is so prevalent that the dysplasia would be expected to be much more frequent than it is.

The following microscopic findings obtained from the first patient might be relevant in regard to the possible pathogenesis of the abnormality.

(1) The course of the dentinal tubules reflecting the backward displacement of the odontoblasts during dentinogenesis changed at the level of the CEJ, as if these cells had attempted to avoid an obstacle. This suggests that the CMD was present in its full extent, when dentin formation arrived at the cervical margin of the crown, i.e., at about 3-4 years of

age.[20] If the development of the CMD were indeed caused by an external insult, this would be predicted to operate relatively early during crown formation, because otherwise first and second primary molars, which complete crown development only during postnatal life,[21] would be expected to exhibit radicular malformations as well.

(2) Outer surfaces of even rudimentary roots were made up of dentin covered by acellular cementum into which inserted PDL fibers. Hence it can be assumed that Hertwig's epithelial root sheath developed more or less normally after the end of amelogenesis. In contrast, the formation of the epithelial bridges which normally give rise to the development of the root furcation, seems to have been impaired. As a consequence, no odontoblasts differentiated and no dentin was laid down below the CMD.

(3) Hard tissue lining the canals of the CMD and the collagen fiber bundles of the constituent soft connective tissue strongly resembled radicular cementum and PDL, respectively. This would indicate that the interglobular components of the CMD were derived from the dental follicle which gives rise to the periodontal tissues.

(4) If the contents of the canals are indeed of follicular origin, the vascular network within the CMD could be derived from the plexus of relatively large blood vessels present at the base of the dental papilla during crown formation.[22,23] Other than the mass of dental mesenchyme which originates from the neural crest, endothelial cells of the follicular blood vessels are derived from mesoderm[24] and, therefore, could well react in a specific way to an external insult. Mesoderm-derived cells proliferate and continuously invade the dental papilla to give rise to the blood vessels of the developing pulp.[24] This process does not seem to have been affected by the formation of the CMD, as the vessel supply of the pulp in the dysplastic teeth appeared normal.

(5) The globules which made up the bulk of the CMD were calcified more densely than peritubular dentin, but seemed to consist of the same mineral as the regular dental hard tissues, i.e., of hydroxyapatite. Furthermore, they lacked collagen fibrils and revealed a concentric lamination. As suggested by the intense staining with alcian blue at pH 2.5 and the fine-granular ultrastructural appearance, they contained large quantities of proteoglycans. In this respect, they resemble the globular calcifications observed in teeth affected by regional odontodysplasia.[25-27] Interestingly, this anomaly has been speculated to be due to damage of the vascular supply, possibly in combination with a viral infection.[7] Similar calcified bodies also occur in some forms of hypoplastic amelogenesis imperfecta, in which the ameloblasts detach from the forming enamel,[28,29] allowing serum and/or tissue fluid to enter the void and to precipitate with mineral.

Therefore, in summary, we propose that the primary target of the early insult eventually leading to the observed root malformation is the vascular plexus at the base of the dental papilla during crown development. As a result of damage to these blood vessels, serum and/or tissue fluid enter the follicular interstitial spaces, where they give rise to the precipitation of calcified globules and finally the formation of the CMD. This ectopic hard tissue plate constitutes a mechanical obstacle for the regular continuation of dentinogenesis and disrupts normal root formation. As to the nature of the early insult, only speculations are possible based on the investigated patients, but the recognition of additional similar cases might help to narrow down the responsible etiological factors.

The authors are grateful to Margrit Amstad-Jossi, Jinan Fierz, and Jacqueline Hofmann-Lobsiger for careful laboratory assistance and skilled preparation of the microscopic sections. They also thank Dr. H. van Waes and Dr. R. Sperling for valuable advice and support.

REFERENCES

1. Andreasen JO. External root resorption: its implication in dental traumatology, paedodontics, periodontics, orthodontics and endodontics. *Int Endod J*. 1985;18:109-118.
2. Tronstad L. Root resorption — etiology, terminology and clinical manifestations. *Endod Dent Traumatol*. 1988;4:241-252.
3. O Carroll MK, Duncan WK, Perkins TM. Dentin dysplasia: review of the literature and a proposed subclassification based on radiographic findings. *Oral Surg Oral Med Oral Pathol*. 1991;72:119-125.
4. Toomarian L, Mashhadiabbas F, Mirkarimi M, Mehrdad L. Dentin dysplasia type I: a case report and review of the literature. *J Med Case Rep*. 2010;4:1-6.
5. Seow WK, Shusterman S. Spectrum of dentin dysplasia in a family: case report and literature review. *Pediatr Dent*. 1994;16:437-442.
6. Tervonen SA, Stratmann U, Mokrys K, Reichart PA. Regional odontodysplasia: a review of the literature and report of four cases. *Clin Oral Investig*. 2004;8:45-51.
7. Gibbard PD, Lee KW, Winter GB. Odontodysplasia. *Br Dent J*. 1973;135:525-532.
8. Jaffe N, Toth BB, Hoar RE, Ried HL, Sullivan MP, McNeese MD. Dental and maxillofacial abnormalities in long-term survivors of childhood cancer: effects of treatment with chemotherapy and radiation to the head and neck. *Pediatrics*. 1984;73:816-823.
9. Sonis AL, Tarbell N, Valachovic RW, Gelber R, Schwenn M, Sallan S. Dentofacial development in long-term survivors of

acute lymphoblastic leukemia. A comparison of three treatment modalities. *Cancer*. 1990;66:2645-2652.
10. Minicucci EM, Lopes LF, Crocci AJ. Dental abnormalities in children after chemotherapy treatment for acute lymphoid leukemia. *Leuk Res*. 2003;27:45-50.
11. Pinzon ML, Gong SG. Arrested root formation of 4 second premolars: report of a patient. *Am J Orthod Dentofac Orthop*. 2012;141:652-656.
12. Luder HU, Amstad-Jossi M. Electron microscopy. In: Kioussi C, ed. *Methods in Molecular Biology*. New York: Springer; 2012:81-93. Odontogenesis − methods and protocols; Vol. 887.
13. Kalk WWI, Batenburg RHK, Vissink A. Dentin dysplasia type I. Five cases within one family. *Oral Surg Oral Med Oral Pathol*. 1998;86:175-178.
14. Steele-Perkins G, Butz KG, Lyons GE, et al. Essential role for NFI-C/CTF transcription-replication factor in tooth root development. *Mol Cell Biol*. 2003;23:1075-1084.
15. Nakatomi M, Morita I, Eto K, Ota MS. Sonic hedgehog signaling is important in tooth root development. *J Dent Res*. 2006;85: 427-431.
16. Han XL, Liu M, Voisey A, et al. Post-natal effect of overexpressed DKK1 on mandibular molar formation. *J Dent Res*. 2011;90:1312-1317.
17. Laisi S, Ess A, Sahlberg C, Arvio P, Lukinmaa PL, Alaluusua S. Amoxicillin may cause molar incisor hypomineralization. *J Dent Res*. 2009;88:132-136.
18. Kumazawa K, Sawada T, Yanagisawa T, Shintani S. Effect of single-dose amoxicillin on rat incisor odontogenesis: a morphological study. *Clin Oral Investig*. 2012;16:835-842.
19. Fält A, Bengtsson T, Kennedy BM, et al. Exposure of infants to budesonide through breast milk of asthmatic mothers. *J Allergy Clin Immunol*. 2007;120:798-802.
20. Moorrees CFA, Fanning EA, Hunt EE Jr. Age variation of formation stages for ten permanent teeth. *J Dent Res*. 1963;42: 1490-1502.
21. Moorrees CFA, Fanning EA, Hunt EE Jr. Formation and resorption of three deciduous teeth in children. *Am J Phys Anthropol*. 1963;21:205-213.
22. Echeverría M. Vascularization of the mandibular tooth germs. *Int Dent J*. 1963;13:446-449.
23. Tobin CE. Blood supply of human fetal teeth. *Am J Anat*. 1971;131:217-225.
24. Rothová M, Feng J, Sharpe PT, Peterková R, Tucker AS. Contribution of mesoderm to the developing dental papilla. *Int J Dev Biol*. 2011;55:59-64.
25. Sapp JP, Gardner DG. Regional odontodysplasia: an ultrastructural and histochemical study of the soft-tissue calcifications. *Oral Surg Oral Med Oral Pathol*. 1973;36:383-392.
26. Gardner DG, Sapp JP. Ultrastructural, electron-probe, and microhardness studies of the controversial amorphous areas in the dentin of regional odontodysplasia. *Oral Surg Oral Med Oral Pathol*. 1977;44:549-559.
27. Kerebel LM, Kerebel B. Soft-tissue calcifications of the dental follicle in regional odontodysplasia: a structural and ultrastructural study. *Oral Surg Oral Med Oral Pathol*. 1983;56: 396-404.
28. Wazen RM, Moffatt P, Francis Zalzal S, Yamada Y, Nanci A. A mouse model expressing a truncated form of ameloblastin exhibits dental and junctional epithelium defects. *Matrix Biol*. 2009;28:292-303.
29. Smith CE, Wazen R, Hu Y, et al. Consequences for enamel development and mineralization resulting from loss of function of ameloblastin or enamelin. *Eur J Oral Sci*. 2009;117: 485-497.

Reprint requests:

Hans Ulrich Luder, DMD, PhD
Breitenloostrasse 29
CH-8708 Männedorf, Switzerland
bhdk.luder@bluewin.ch